# Drop Formation at Low Velocities in Liquid-Liquid Systems:

**GEORGE F. SCHEELE and BERNARD J. MEISTER**

**Cornell University, Ithaca, New York**

## Part I. Prediction of Drop Volume

**A correlation is presented for predicting the drop volume for injection at low velocities of one Newtonian liquid into a second stationary immiscible Newtonian liquid in the absence of surface active agents. The analysis, which is based on a two-stage process of drop formation, predicts drop volumes within an average error of 11% for fifteen liquid-liquid systems covering a wider range of variables than any previous study. Although the equation was tested primarily with mutually saturated liquids, it correctly predicted drop size for two systems where mass transfer was occurring.**

The prediction of the interfacial area formed when one liquid is injected into a second immiscible liquid through a single orifice or nozzle is necessary for calculations of heat and mass transfer rates in such processes. This paper considers the low flow velocity region prior to jet formation where uniform size drops are formed directly at the nozzle tip and break off in a regular pattern. Hayworth and Treybal (5) and Null and Johnson (8) both present photographs which illustrate the drop formation process.

Harkins and Brown (4) derived an expression for calculating the drop volume at negligibly small flow rates by equating the buoyancy and interfacial tension forces and correcting the volume for the fraction of liquid which remains attached to the nozzle after drop break off.

For cases where velocity effects become important there are two widely accepted correlations. Hayworth and Treybal (5) extended the analysis of Harkins and Brown by incorporating into the force balance the inertial and drag forces which arise for finite injection velocities, while Null and Johnson (8) used a geometric approach to obtain a correlation for drop volumes.

Rao et al. (10) have recently developed a correlation based on a two-stage drop formation process. In the static stage the drop is assumed to expand until the buoyant force balances the interfacial tension force. The drop volume at the end of the static stage is given by the equation of Harkins and Brown. During the second stage, when the drop is detaching from the nozzle, the drop continues to grow.

Meister (7) found that the Hayworth-Treybal and Null-Johnson correlations did not satisfactorily predict drop size over the wide range of liquid properties and nozzle diameters he studied, a result consistent with the observations of Null and Johnson (8), who found maximum average errors of 94 and 377% when they compared experimental data with their analysis and that of Hayworth and Treybal, respectively.

Although Rao et al. indicate that their analysis significantly reduces the error for many systems (10), it has some weaknesses, the most evident of which is its inability to predict a drop volume smaller than that given by the Harkins and Brown analysis. Drops of smaller than static condition size were observed in this study.

This paper presents an improved correlation for drop volume based on the two-stage drop formation process and extensive experimental data.

### EXPERIMENTAL STUDY

Although several sets of drop volume data exist in the literature (5, 8, 10), it was felt that additional experiments were necessary to obtain a better understanding of the mechanism of drop formation and to provide a more stringent test of any proposed correlation by extending the range of variables studied. Experiments were designed to obtain drop diameter as a function of injection velocity and nozzle diameter for systems with a wide range of physical properties. In all systems the dispersed phase was of lower density than the continuous phase.

The experimental apparatus is shown schematically in Figure 1. The test section consisted of a continuous phase tank, into whose bottom the desired nozzle was fastened. The tank,

Bernard J. Meister is with The Dow Chemical Company, Midland, Michigan.

rectangular to minimize optical distortion, was 2½ ft. high and had a square cross section 1 ft. on each side. Data obtained by Shiffler (*11*) show that wall effects are negligible in a tank with a 1 ft. square cross section. Three sides of the tank were plate glass, and the fourth side and bottom were brass plate. The dispersed phase feed and hold tanks and valves were type 304 stainless steel, and all tubing was copper to eliminate contamination of the liquid.

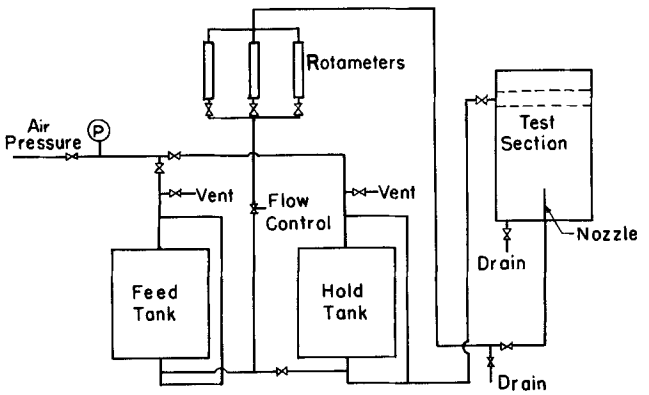


**Fig. 1. Schematic diagram of experimental apparatus.**

The five nozzles used were made of stainless steel tubing 4 ft. long and had inside diameters ranging from 0.0813 to 0.688 cm. The large length to diameter ratios, which ranged from 177 for the largest nozzle to 1,500 for the smallest, were chosen to minimize disturbances and to assure a fully developed velocity profile at the nozzle exit. The nozzle tips were machined flat so that undesirable wetting of a nozzle by the dispersed phase could be detected easily. Data were obtained only from experiments in which no wetting occurred.

Regulated laboratory compressed air was used to circulate the dispersed phase liquid. The dispersed phase flow was controlled with a needle valve having a vernier scale, and its rate was measured with the calibrated rotameter of appropriate capacity.

Drop diameters were measured from still photographs taken with a Praktina FX 35-mm. camera using Tri X panchromatic film and a shutter speed of $10^{-3}$ sec. Four photographs were taken for each experimental condition, and each photograph contained images of several drops. Drop sizes were measured from the negatives with a microfilm reader. If the drop was deformed from a spherical shape, the drop diameter was recorded as the arithmetic average of the major and minor diameters. Christiansen (*3*) has shown that this procedure causes less than 5% error in the calculation of drop volume if the ratio of major to minor diameters is less than 1.7. In this study the ratio was less than 1.2 for most drops. In twelve of the 600 experiments satellite drops were formed from the neck of the drop breaking away from the nozzle. These drops were ignored in the calculation of drop volume because they contributed negligibly to the interfacial area. These drops did not affect the uniformity of the primary drops because, on occasions when they were formed, one satellite drop was formed with each primary drop.

To study the mechanism of drop formation high-speed motion pictures were taken with a Wollensak Fastax WF3 camera at a rate of 2,500 frames/sec. with 4X panchromatic film.

The dispersed phase was dyed with Calco Oil Red to improve the contrast in the photographs. This dye is recommended by Kintner (*6*) because it has no effect on the interfacial tension and is devoid of other interfacial activity for organic liquid-water systems.

The experimentally measured physical properties of the liquid pairs investigated are presented in Table 1. Systems 1 through 13 were mutually saturated by mixing the phases together prior to study and measurement of properties. Systems 14 and 15 were not mutually saturated because they were used to study the effect of mass transfer on the drop formation process. Viscosities were measured with Cannon-Fenske viscometers, densities were determined with a set of Elmer and Ahmid hydrometers, and interfacial tensions were obtained with the Harkins-Brown drop volume technique.

## THEORY

### Force Balance

There are four major forces which act on a drop during the process of formation at a nozzle. The buoyancy force due to the density difference between the two fluids and the inertial or kinetic force associated with fluid flowing out of the nozzle act to separate the drop from the nozzle, while the interfacial tension force at the nozzle tip and the drag force exerted by the continuous phase act to keep the drop on the nozzle. When the lifting force exceeds the restraining force, the drop begins to break away from the nozzle.

If $V_{FS}$ is the total liquid volume attached to the nozzle tip at the instant the net force on the forming drop equals zero, the buoyancy force is

$$F_B = V_{FS} g \Delta\rho \tag{1}$$

The interfacial tension force is

$$F_S = \pi\sigma D_N \tag{2}$$

At static conditions these are the only forces acting on the drop, and the volume $V_F$ of a drop formed is given by

$$V_F = \frac{F\pi\sigma D_N}{g\Delta\rho} \tag{3}$$

where $F$ is the Harkins-Brown factor which corrects for the fraction of the liquid volume which remains attached to the nozzle after drop break off.

In any practical process velocity effects become significant. If it is assumed that all the energy in the fluid leaving the nozzle is transmitted in the vertical direction to the forming drop, the kinetic force can be formulated. The differential kinetic force acting on a differential cross-sectional area is

$$dF_K = \rho' U_Z^2 dA \tag{4}$$

In the present experiments a straight section of more than 100 pipe diameters preceeded the nozzle exit, and the Reynolds number in the nozzle was always less than 2,100, so that the parabolic velocity distribution

$$U_Z = 2U_N \left[ 1 - \left( \frac{R}{R_N} \right)^2 \right] \tag{5}$$

can be substituted into Equation (4). Integration over the nozzle area gives

$$F_K = \frac{4}{3} \rho' Q U_N \tag{6}$$

The drag force is more difficult to evaluate. The simplest approach is to consider the forming drop as a sphere with a velocity $U_F$ relative to the continuous phase at the instant the net force is zero. By definition

$$F_D = \frac{C_D \pi\rho U_F^2 (D_{FS})^2}{8} \tag{7}$$

where $D_{FS}$ is the diameter of the attached drop at the instant the forces are in balance.

Results of this study show that in all systems where $F_D$ is significant the drop Reynolds number is less than 1.0 because of large continuous phase viscosity. If the drop is treated as a solid sphere, the drag coefficient is given by

$$C_D = \frac{24\mu}{D_{FS} U_F \rho} \tag{8}$$

and the drag force becomes

$$F_D = 3\pi\mu U_F D_{FS} = \frac{3\pi\mu U_F D_F}{F^{1/3}} \tag{9}$$

Although the drop velocity is a variable function of position, it is assumed that $U_F$ can be approximated by the leading edge velocity of the drop. For a drop that maintains a spherical shape throughout its growth period, the time elapsed during drop formation is

$$t = \frac{\pi(h^3 - h_o^3)}{6Q} \tag{10}$$

where $h$ is the distance from the nozzle tip to the leading edge of the drop and $h_o$, the diameter of the liquid left on the nozzle after drop break off, is related to the diameter $D_F$ of the drop formed by the Harkins-Brown correction factor $F$:

$$h_o^3 = \frac{D_F^3(1-F)}{F} \tag{11}$$

The leading edge velocity of the drop is

$$\frac{dh}{dt} = \frac{2Q}{\pi}\left(\frac{6Qt}{\pi} + D_F^3\frac{(1-F)}{F}\right)^{-2/3} \tag{12}$$

At the instant the forces are in balance

$$U_F = \left(\frac{dh}{dt}\right)_{t=t_F} \tag{13}$$

where

$$t_F = \frac{\pi D_F^3}{6Q} \tag{14}$$

Equation (14) assumes that at the instant the net force becomes zero a drop of diameter $D_F$ breaks off the nozzle. Substitution of Equation (14) into Equation (12) yields

$$U_F = \frac{2QF^{2/3}}{\pi D_F^2} \tag{15}$$

and Equation (9) for the drag force becomes

$$F_D = \frac{6\mu Q F^{1/3}}{D_F} \tag{16}$$

Equation (16) is valid only when the assumption of spherical growth is justified. Figure 2 shows that Equation (12) gives a good prediction of the leading edge velocity measured experimentally from high-speed movies for the smallest nozzle used. However, for larger diameter nozzles there was drop deformation which caused a larger forward velocity than predicted by Equation (12). This deformation appeared to be primarily a function of the ratio of the nozzle diameter to the drop diameter. Since the Harkins-Brown correction factor is also a function of this ratio, the drag force can be generalized to

$$F_D = K_D\frac{\mu Q}{D_F}\left(\frac{D_N}{D_F}\right)^n \tag{17}$$

where $K_D$ and $n$ must be evaluated from experimental data. The empiricism also corrects for any reduction in $F_D$ due to induced continuous phase motion.

At equilibrium

$$F_B + F_K = F_S + F_D \tag{18}$$

Substituting the appropriate expressions for the forces and rearranging, one gets

$$V_{FS} = \frac{\pi\sigma D_N}{g\Delta\rho} + \frac{K_D\mu Q}{D_F\, g\Delta\rho}\left(\frac{D_N}{D_F}\right)^n - \frac{4\rho' Q U_N}{3g\,\Delta\rho} \tag{19}$$

Equation (19) gives the volume of liquid on the nozzle tip at equilibrium. If the drop instantaneously broke off, multiplication of Equation (19) by $F$ would give the volume of the separated drop. However, it was observed in high-speed movies that a considerable amount of liquid flowed into a drop during the process of drop break off after the net lifting forces exceeded the net restraining forces. As the nozzle velocity increased, this mechanism

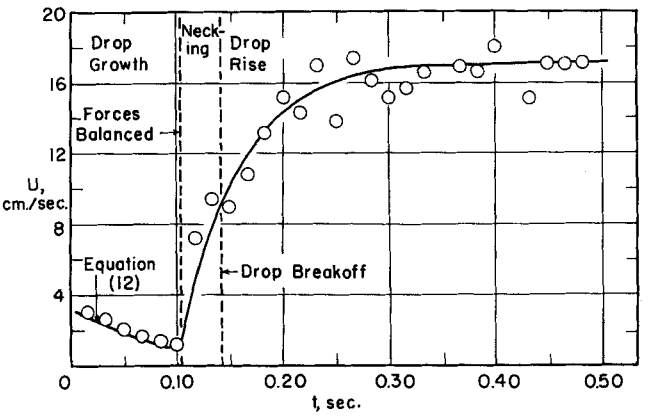


**Fig. 2. Leading edge velocity of drop as function of time for injection of heptane into water through 0.0813 cm. diameter nozzle at nozzle velocity = 35.2 cm./sec.**

contributed a greater and greater proportion of the final drop volume. Siemes and Kauffmann (*12*) observed this phenomenon for gases injected into liquids, and Rao *et al.* (*10*) postulated the mechanism for liquids injected into liquids. To predict $V_F$ it is necessary to estimate this additional flow.

#### Flow Into Drop During Necking

The additional volumetric flow $V_{FN}$ out of the nozzle during the process of drop break off can be calculated from the equation

$$V_{FN} = Qt_B \tag{20}$$

if the time $t_B$ for drop necking to occur is known. If the initial neck diameter is assumed equal to the nozzle diameter, $t_B$ is given by the equation

$$\int_{R_N}^{o} dR = -\int_o^{t_B} U_R\, dt \tag{21}$$

where $U_R$ is the radial necking velocity during drop break off.

Instead of developing a complex analysis for $U_R$, limited experimental data on $U_R$ were coupled with an approximate functional relationship for the vertical rise velocity $U_V$ to obtain a simplified expression for $U_R$.

Once the process of necking has begun, a differential force balance on the drop can be written as

$$m\frac{dU_V}{dt} = Qtg\Delta\rho - 3\pi\mu D_F U_V \tag{22}$$

if the following are assumed:

1. $U_V\, dm/dt$ is negligible compared with the acceleration term.
2. The change in interfacial tension and kinetic energy forces during necking is negligible.
3. All the additional flow $Qt$ from the nozzle enters the drop during necking.
4. $U_V$ is in the Stokes law region.
5. An average value of $D_F$ can be used in the drag term.
6. $U_F$ is negligibly small.

If the steady state rise velocity after drop break off and the drop formation time are used as the characteristic velocity and time, respectively, dimensionless velocity and time variables are defined by

$$U_V' = 18\,\mu U_V/D_F^2 g\Delta\rho \qquad (23a)$$

$$t' = 6\,Qt/\pi\,D_F^3 \qquad (23b)$$

and Equation (22) can be written in dimensionless form as

$$\frac{dU_V'}{dt'} + \frac{3\pi^2\,\mu D_F U_V'}{Q\rho'} = \frac{3\pi^2\,\mu D_F t'}{Q\rho'} \qquad (24a)$$

If the approximate boundary conditions

$$U_V' = 0 \text{ at } t' = t_o' \qquad (24b)$$

$$U_V' = 1.0 \text{ at } t' = 1.0 \qquad (24c)$$

are valid and the same percentage of total drop formation time is involved in the necking process for all experimental conditions, $U_V'$ will be a function only of $t'$ and the dimensionless group $\mu D_F/Q\rho$. Although the data do not fully support this approximation, any more complex approach unnecessarily complicates the final drop volume correlation.

It is assumed that the dimensionless radial necking velocity $U_R'$ depends on the same parameters as $U_V'$. High-speed movies of droplet formation in the heptane-water system with the largest nozzle, where the time duration of necking was sufficiently long to measure the time dependence of $U_R$, showed that the data fit the equation

$$U_R = Kt^2 \qquad (25)$$

A generalized equation consistent with the above equation is

$$U_R' = K_1\left(\frac{\mu D_F}{Q\rho'}\right)^a t'^2 \qquad (26)$$

Solving for $K$ one gets

$$K = K_2\frac{Q^2 g\Delta\rho}{DF^4\mu}\left(\frac{D_F\mu}{Q\rho'}\right)^a \qquad (27)$$

To simplify the final correlation for drop volume, $a$ was arbitrarily set equal to 1.0 so that viscosity would appear only in the drag term, and $D_F^3$ was approximated by $6\sigma\,D_N/g\Delta\rho$. Combining Equations (20), (21), (25), and (27), one obtains

$$V_{FN} = K_3\left(\frac{Q^2 D_N^2\rho'\sigma}{(g\,\Delta\,\rho)^2}\right)^{1/3} \qquad (28)$$

Experimental observations indicated that part of the nozzle throughput during necking does not go into the drop. It will be assumed that the fraction which does flow into the drop is equal to the Harkins-Brown correction factor $F$, since this simplifies the form of the final equation.

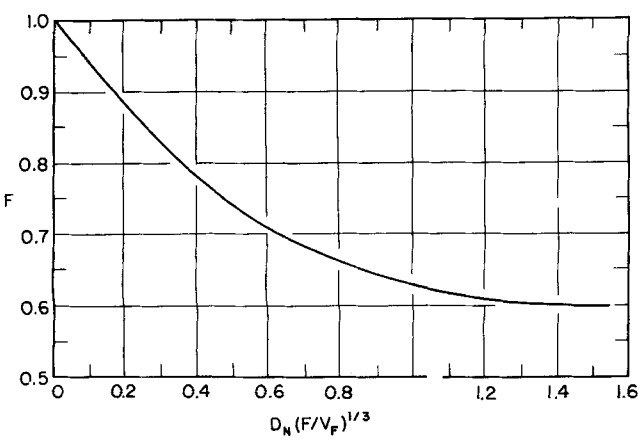


Fig. 3. Harkins-Brown correction factor $F$ for use in Equation (30).

#### Final Correlation

The drop volume after break off is given by

$$V_F = F\,(V_{FS} + V_{FN}) \qquad (29)$$

After substitution of Equations (19) and (28) for $V_{FS}$ and $V_{FN}$, respectively, the undetermined coefficients and exponent were evaluated by using experimental drop volume data. $K_3$ was determined by fitting all the data for systems with continuous phase viscosity less than 10 centipoises, since for these systems the drag term was negligible. This value of $K_3$ was then used with the heptane-glycerine data to obtain $K_D$ and $n$. The final correlation is

$$V_F = F\left[\frac{\pi\sigma\,D_N}{g\Delta\rho} + \frac{20\mu Q\,D_N}{D_F^2 g\Delta\rho} - \frac{4\rho'\,QU_N}{3g\Delta\rho} + 4.5\left(\frac{Q^2 D_N^2\rho'\sigma}{(g\Delta\rho)^2}\right)^{1/3}\right] \qquad (30)$$

Although the constants were obtained only from data in which the dispersed phase was less dense than the continuous phase, the theoretical analysis should also be valid in the reverse situation so long as the injection is in the vertical plane. The only difference in the two situations is the direction of the pressure gradient in the continuous phase relative to the direction of dispersed phase injection.

The Harkins-Brown correction factor $F$ is generally presented as a plot of $F$ vs. $D_N/(V_F)^{1/3}$. This plot, although useful in interfacial tension determinations, is not convenient for use with Equation (30) because the drop volume is not known. Therefore the correction factor has been replotted as $F$ *vs.* $D_N(F/V_F)^{1/3}$ in Figure 3. The quantity $D_N(F/V_F)^{1/3}$ can be calculated directly from Equation (30) when the drag term is negligible. For continuous phase viscosities greater than 10 centipoises the drag term is not negligible and the solution becomes a trial-and-error one. As originally derived, $D_F$ in the drag term was the drop diameter when the flow into the drop during necking was negligible. To simplify the final equation, however, the drag term was evaluated by using the experimental drop diameter, so $D_F$ in Equation (30) is the actual drop diameter.

Equation (30) was derived for a parabolic velocity profile in the liquid leaving the nozzle. For a flat velocity profile, the equation should be valid if the constant 4/3 in the kinetic term is replaced by 1.0.

## EXPERIMENTAL RESULTS

Equation (30) was used to calculate drop volumes for all systems listed in Table 1. All the nozzles were used with the heptane-water system, but for many systems only one nozzle was studied. For each system and nozzle, drop volumes were calculated for three or four flow rates spanning the velocity region prior to jet formation. These computed values were compared with the experimental volumes, and a percentage error was obtained by dividing the deviation of the calculated from the experimental volume by the smaller of the two values; in this way a calculated drop volume which is half the actual volume has the same error as one twice the experimental volume.

The mean percentage deviation for seventy-eight runs with Equation (30) was 11.0%, and in only two runs was the error greater than 30%. For the same data the Hayworth-Treybal and Null-Johnson predictions had mean per-

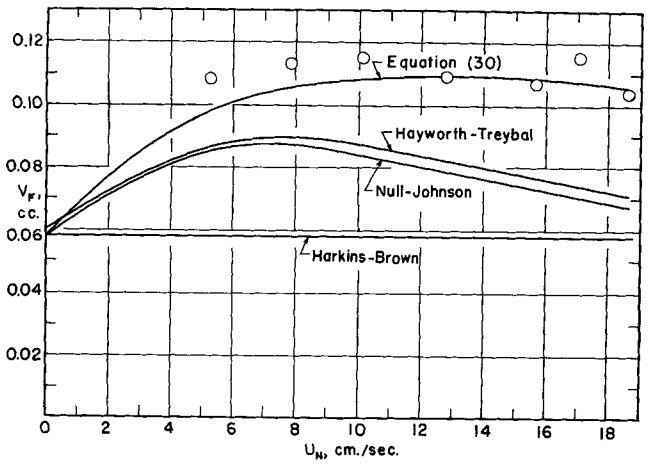


Fig. 4. Drop volume nozzle velocity dependence for heptane injection into water. Nozzle diameter = 0.254 cm.

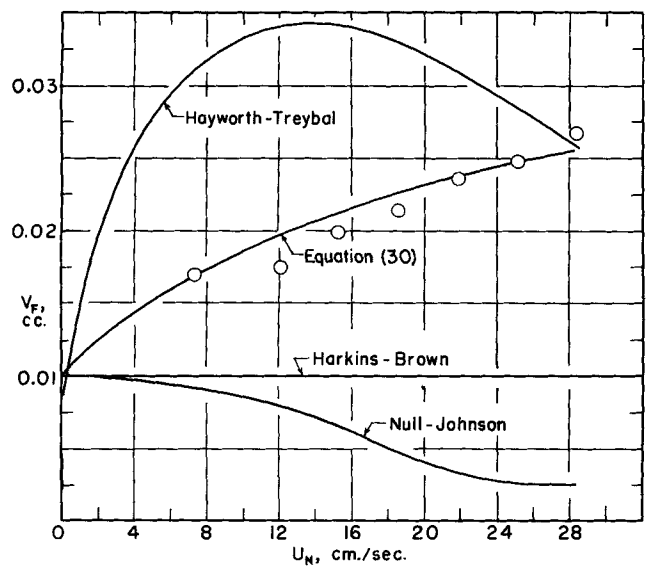


Fig. 5. Drop volume nozzle velocity dependence for heptane injection into glycerine. Nozzle diameter = 0.0813 cm.

centage deviations of 83.3 and 139.5%, respectively. Comparisons of experimental data with the predictions of Equation (30) and the Hayworth-Treybal and Null-Johnson correlations are presented for four representative systems in Figures 4 to 7. Comparisons were not made with the analysis of Rao *et al.* because it cannot predict experimental results such as those shown in Figure 7 where the drop volume becomes smaller than that predicted by the Harkins-Brown equation.

The errors obtained by using Equation (30) show no trend with physical properties, and the mass transfer results are correlated as satisfactorily as data for the mutually saturated systems. There is, however, a trend to negative errors for small diameter nozzles and low flow rates and positive errors for large nozzles and high flow rates.

## DISCUSSION OF RESULTS

The drop volume correlation given by Equation (30) is more accurate than previous correlations over a wider range of physical properties. It is also easier to use, especially when the continuous phase viscosity is less than 10 centipoises.

A primary reason for the improvement is that several of the liquid-liquid pairs employed in the experimental

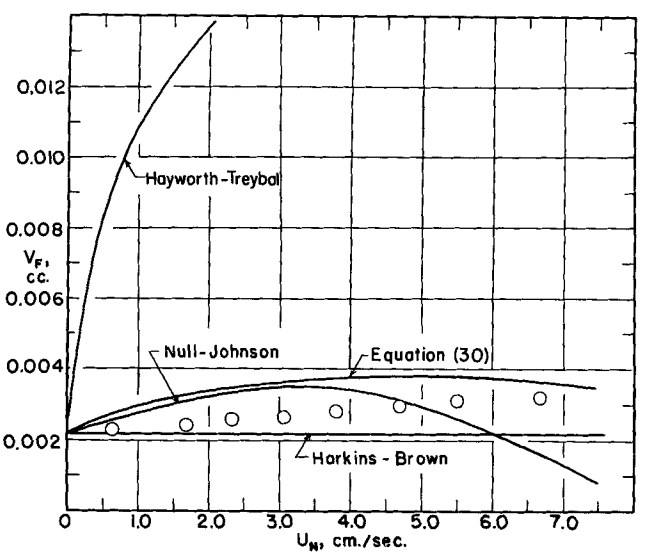


Fig. 6. Drop volume nozzle velocity dependence for butyl alcohol injection into water. Nozzle diameter = 0.0813 cm.

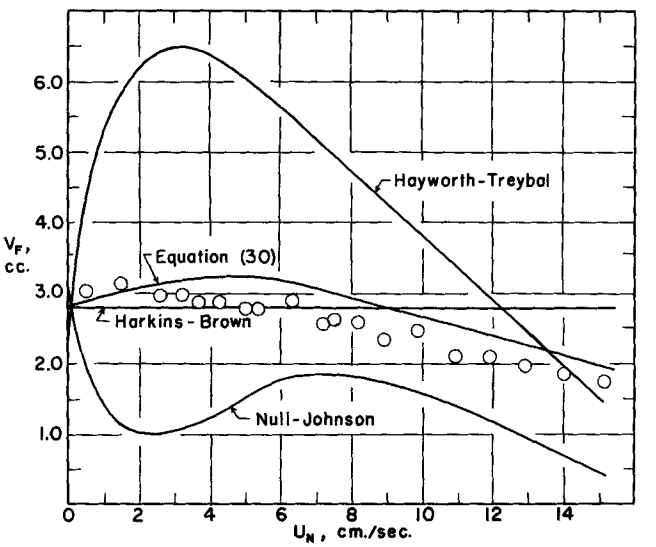


Fig. 7. Drop volume nozzle velocity dependence for 55% carbon tetrachloride-45% heptane injection into water. Nozzle diameter = 0.254 cm.

investigation afford a stringent test of any model because of extreme values of phase viscosities, interfacial tension, or density difference. While both the Hayworth-Treybal and Null-Johnson correlations show good agreement with experimental data at times, they are sufficiently empirical that they can't be safely extrapolated beyond the range of variables for which they were established. That this range is quite limited is shown by the fact that although several of the systems in the present study have fairly common physical properties, only two of the twenty-five system-nozzle combinations studied have all their variables within the range studied by Null and Johnson, and none have all their variables within the range covered by the Hayworth and Treybal correlation.

Figures 5 and 6 illustrate the difficulty of extrapolating empirical correlations. Null and Johnson did not study systems with a highly viscous continuous phase and so did not include in their analysis the effect of viscous drag in increasing drop volume. For this reason their correlation was unsatisfactory when applied to the glycerine series of experiments, as can be seen in Figure 5. Hayworth and Treybal used a synthetic wetting agent to

Table 1. Physical Properties of Experimental Systems

| System No. | Dispersed phase | Density, g./cc. | Viscosity, centipoises | Continuous phase | Density, g./cc. | Viscosity, centipoises | Interfacial tension, dyne/cm. |
|---|---|---|---|---|---|---|---|
| 1 | Heptane | 0.683 | 0.393 | Water | 0.996 | 0.958 | 36.2 |
| 2 | Heptane | 0.683 | 0.393 | Glycerine | 1.254 | 515.0 | 26.3 |
| 3 | Heptane | 0.683 | 0.393 | 90% Glycerine 10% Water | 1.236 | 168.0 | 25.1 |
| 4 | Heptane | 0.683 | 0.393 | 80% Glycerine 20% Water | 1.224 | 78.5 | 22.8 |
| 5 | Heptane | 0.683 | 0.393 | 70% Glycerine 30% Water | 1.190 | 21.9 | 24.5 |
| 6 | Heptane | 0.683 | 0.393 | 50% Glycerine 50% Water | 1.143 | 6.95 | 26.0 |
| 7 | Butyl alcohol | 0.836 | 2.52 | Water | 0.990 | 1.09 | 1.79 |
| 8 | 55% $CCl_4$ 45% Heptane | 0.986 | 0.488 | Water | 0.996 | 0.958 | 32.0 |
| 9 | Paraffin oil | 0.876 | 121.0 | Water | 0.996 | 0.958 | 43.4 |
| 10 | 90% Paraffin oil 10% Heptane | 0.865 | 35.3 | Water | 0.996 | 0.958 | 44.4 |
| 11 | 80% Paraffin oil 20% Heptane | 0.843 | 15.7 | Water | 0.996 | 0.958 | 45.4 |
| 12 | 70% Paraffin oil 30% Heptane | 0.822 | 6.71 | Water | 0.996 | 0.958 | 44.8 |
| 13 | Benzene | 0.871 | 0.544 | Water | 0.996 | 0.958 | 31.2 |
| 14 | Benzene | 0.871 | 0.544 | 95% Water 5% Acetone | 0.990 | 1.04 | 20.2 |
| 15 | 95% Benzene 5% Acetone | 0.870 | 0.552 | Water | 0.996 | 0.958 | 20.2 |

Note: Percents are only approximate and are by weight.

lower the interfacial tension in their studies. The effect of surfactant addition cannot be characterized solely by the resultant equilibrium interfacial tension lowering because for a given surfactant concentration the interfacial tension increases with increasing velocity through the nozzle as a result of the slow diffusion of surfactant to the interface. This causes a much greater increase in drop volume with increasing nozzle velocity than is observed for pure liquids. Thus, Hayworth and Treybal's interfacial tension dependency will cause appreciable error when the correlation is applied to pure systems with low interfacial tensions, as shown in Figure 6 for the butyl-alcohol-water system. Conversely, Equation (30) should not be applied to systems containing surfactants.

The correlation given by Equation (30) also suffers from empiricism. The weak point in the analysis is the term for predicting flow into the drop during necking. The assumptions, based on very limited data, are at best approximate and are the reason the errors show a trend with both nozzle diameter and injection velocity. There is no guarantee that the correlation can be extrapolated to regions of variables not investigated. However, fitting the parameters to experimental data obtained from systems having such a wide range of physical properties assures that the correlation will satisfactorily predict drop volumes in many systems.

Another reason for the success of the present correlation is the consideration that flow into the drop during the necking process can contribute significantly to the final drop volume and must be treated independently. Any empirical incorporation of this phenomenon into one of the force terms will cause errors in the dependence of drop volume on flow rate, nozzle diameter, and physical properties, as can be seen from Equation (30). The only previous analysis to separate out this effect is that of Rao et al. (*10*), who proposed two models for flow into the drop during the detachment process, one for low viscosity and one for high viscosity continuous phase liquids. For large viscosity liquids the analysis predicts that the additional volumetric flow $V_{FN}$ into the drop during the break off process will be

$$V_{FN} = K_4 \left[ \frac{\mu^{3/2} D_N \sigma Q^{3/2}}{(g\Delta\rho)^{5/2}} \right]^{1/3} \tag{31}$$

In spite of the similarity between Equations (31) and (28), the analysis of Rao et al. differs significantly from the present one because it considers that the static drop volume prior to necking can be obtained by equating the buoyant and interfacial tension forces rather than from the more general force balance given by Equation (18). There is experimental support for including the kinetic force term in the initial force balance, because drop volumes smaller than the static drop volume predicted by Rao et al. do detach from the nozzle. The data shown in Figure 7 illustrate this for a system where the density difference between the phases is small. The upward kinetic force leads to the start of necking at a smaller drop volume than would be predicted from a balance of buoyant and interfacial tension forces, and even the additional flow into the drop during the detachment process does not create a drop as large as that predicted by Rao et al. for the static drop. There is no photographic evidence in the present study that the necking mechanism depends on continuous phase viscosity. Rather, there appears to be only one mechanism. It is probably the neglect of the drag force in the initial force balance which makes it necessary to postulate a second mechanism to account for the increasing importance of drag with increasing continuous phase viscosity.

Because the purpose of many liquid-liquid systems is to transfer solute from one phase to the other, some experiments were performed to determine the effect of mass transfer on Equation (30), which was established from data for mutually saturated phases. Experiments used the benzene-acetone-water system because, at low concentrations of acetone, the distribution coefficient of acetone between benzene and water is approximately 1.0 on a

weight percent basis for concentrations below 10% acetone (9). Therefore, the driving force for transfer into or out of the jet for a given concentration of acetone in one of the phases is approximately the same. The concentration of 5% by weight acetone was used. The interfacial tension was reduced from 31.2 dynes/cm. for benzene-water to 20.2 dynes/cm. when the benzene and water each contained 5% by weight acetone at equilibrium.

The drop volume was smaller for the mass transfer systems than for the saturated benzene-water system. Equation (30) predicted the drop volumes for mass transfer when the equilibrium interfacial tension for 5% by weight acetone in each phase was used. These results indicate that for this system the effective interfacial tension was equal to the equilibrium interfacial tension over the velocity range investigated. The subject of effective interfacial tension has been extensively studied (*1* to *3*), and it has been shown that the main variables are the rate of surface renewal and the solute molecular size. It appears that the acetone molecule was small enough that its diffusion rate was sufficient to maintain the equilibrium interfacial tension.

Therefore, if the solute is of small molecular size and its concentration is low, Equation (30) can be applied to mass transfer systems if the equilibrium interfacial tension is used. The equation predicts only the drop size leaving the nozzle, and it does not include coalescence effects in the continuous phase above the nozzle.

## NOTATION

$A$ = cross-sectional area of nozzle, sq. cm.
$a$ = exponent as defined by Equation (26)
$C_D$ = drag coefficient
$D_F$ = diameter of detached drop, cm.
$D_{FS}$ = diameter of attached drop at instant forces are in balance, cm.
$D_N$ = nozzle inside diameter, cm.
$F$ = Harkins-Brown correction factor
$F_B$ = buoyant force, dynes
$F_D$ = drag force, dynes
$F_K$ = kinetic force, dynes
$F_S$ = interfacial tension force, dynes
$g$ = acceleration of gravity, 980 cm./sec.$^2$
$h$ = distance from nozzle tip to leading edge of drop, cm.
$h_o$ = diameter of liquid left on nozzle after drop break off, cm.
$K$ = numerical coefficient in several equations
$m$ = mass of drop, g.
$n$ = exponent in Equation (17)
$Q$ = volume flow rate of dispersed phase, cc./sec.
$R$ = radius of neck of drop, cm.
$R_N$ = nozzle radius, cm.
$t$ = time, sec.
$t'$ = dimensionless time, defined by Equation (23*b*)
$t_B$ = time duration of drop necking, sec.
$t_F$ = time required for forces to reach equilibrium, sec.
$U_F$ = velocity of the forming drop at the instant necking starts, cm./sec.
$U_N$ = dispersed phase average velocity through the nozzle, cm./sec.
$U_R$ = radial necking velocity, cm./sec.
$U_R'$ = dimensionless radial necking velocity
$U_V$ = vertical rise velocity during necking, cm./sec.
$U_V'$ = dimensionless vertical rise velocity during necking, as defined by Equation (23*a*)
$U_Z$ = local dispersed phase velocity in the nozzle, cm./sec.
$V_F$ = drop volume after break off from the nozzle, cc.
$V_{FS}$ = liquid volume attached to the nozzle when necking starts, cc.
$V_{FN}$ = volumetric flow out of the nozzle during necking, cc.
$\mu$ = continuous phase viscosity, g./(cm.)(sec.)
$\rho, \rho'$ = densities of continuous and dispersed phases, respectively, g./cc.
$\sigma$ = interfacial tension, dyne/cm.

## LITERATURE CITED


1. Addison, C. C., and T. A. Elliott, *J. Chem. Soc.*, 2788 (1949).
2. *Ibid.*, 3090 (1950).
3. Christiansen, R. M., Ph.D. thesis, Univ. Pennsylvania, Philadelphia (1955).
4. Harkins, W. D., and F. E. Brown, *J. Am. Chem. Soc.*, **41**, 499 (1919).
5. Hayworth, C. B., and R. E. Treybal, *Ind. Eng. Chem.*, **42**, 1174 (1950).
6. Kintner, R. C., T. J. Horton, R. E. Graumann, and S. Amberkar, *Can. J. Chem. Eng.*, **39**, 235 (1961).
7. Meister, B. J., Ph.D. thesis, Cornell Univ, Ithaca, N. Y. (1966).
8. Null, H. R., and H. F. Johnson, *AIChE J.*, **4**, 273 (1958).
9. Othmer, D. F., R. E. White, and Edward Trueger, *Ind. Eng. Chem.*, **33**, 1240 (1941).
10. Rao, E. V. L. N., R. Kumar, and N. R. Kuloor, *Chem. Eng. Sci.*, **21**, 867 (1966).
11. Shiffler, D. A., Ph.D. thesis, Cornell Univ., Ithaca, N. Y. (1965).
12. Siemes, W., and J. F. Kauffman, *Chem. Eng. Sci.*, **5**, 127 (1956).



*Manuscript received February 13, 1967; revision April 26, 1967; paper accepted May 22, 1967.*


# Part II. Prediction of Jetting Velocity


**Equations are derived for predicting the velocity above which a jet forms when one Newtonian liquid is injected into a second stationary immiscible liquid. Comparison of the theory with experimental data obtained for fifteen liquid-liquid systems and five nozzle diameters shows a mean error of 6.6%. The equation also predicts the jetting velocity for injection of liquids into gases and the critical velocity at which bubble formation changes from a constant volume to a constant frequency mechanism for gas injection into liquids.**


The drop volume correlation developed in Part I applies only at low velocities where drops form directly at the nozzle. As the flow rate through the nozzle is increased, a critical velocity called the *jetting velocity* is reached, above which a jet of liquid issues from the nozzle. The jet breaks into drops, but, because the drop formation mechanism has changed, the drop size can no longer be predicted by the low velocity correlation. To define the region of applicability of the low velocity drop volume equation, it is necessary to predict the jetting velocity.